# *Comptes Rendus*

## *Géoscience*

### *Sciences de la Planète*

Michel Condomines, Olivier Bruguier, Inès Hajji and Chedia Zaara-Ben Mosbah

**Unusual open-system behaviour revealed by LA-MC-ICP-MS U–Th dating of coral and coralline algae bio-carbonates**

Research article — Geochemistry, cosmochemistry

# Unusual open-system behaviour revealed by LA-MC-ICP-MS U–Th dating of coral and coralline algae bio-carbonates

**Michel Condomines**[*, a]**, Olivier Bruguier**[®] [a]**, Inès Hajji** [b]
**and Chedia Zaara-Ben Mosbah**[†, b]

[a] Géosciences Montpellier, Université de Montpellier, CNRS UMR 5243, France

[b] Laboratoire des Ressources Minérales et Environnement-Département de Géologie, Faculté des Sciences de Tunis, Université Tunis El Manar, Tunisie

*E-mails:* michel.condomines@umontpellier.fr (M. Condomines), olivier.bruguier@umontpellier.fr (O. Bruguier), ineshajji1990@gmail.com (I. Hajji)

**Abstract.** This paper presents new U–Th ages obtained by LA-MC-CP-MS (laser ablation - multi-collector - inductively coupled plasma - mass spectrometry) on coral samples from a sedimentary core of the Tunis lagoon. The ages and calculated $(^{234}U/^{238}U)_0$ initial ratios, similar to the seawater value for most corals demonstrate that they behaved as closed systems, or with only a very limited loss of $^{234}U$ and $^{230}Th$. The ages (from 196 to 182 ka) show that the coral-rich sediments were deposited near the end of isotope stage 7. The precision on the dates is comparable to those of alpha-spectrometry (around 7.6% on average), but the possibility of multiple *in-situ* analyses offers other advantages. An example is provided by the very unusual open-system behaviour found in the outer Mg-calcite border of a coral branch, formed by a coralline red alga. The very high $(^{234}U/^{238}U)$ and $(^{230}Th/^{238}U)$ activity ratios (1.41 and 2.04, respectively) are tentatively explained using the model proposed by Thompson et al. [2003], that involves continuous enrichment of $^{234}Th$ $(^{234}U)$ and $^{230}Th$ recoil nuclei provided by an U-enriched source. We suggest that this source might come from the bio-mineral itself, in the form of organic matter originally involved in the encrusting algal activity, and eventually degraded with an almost complete U-loss.

**Keywords.** *In situ* U–Th dating of corals, LA-MC-ICP-MS, Open-system model, Recoil nuclei, Coralline red algae.

---

[*] Corresponding author.

[†] Deceased.

## 1. Introduction

The so-called U–Th method ($^{238}$U–$^{234}$U–$^{230}$Th) has long been one of the most useful dating methods for carbonates formed during the last 500–600 ka. The development of mass spectrometry and in particular the advent of multi-collector, plasma source mass spectrometers (MC-ICP-MS) has resulted in an extreme precision in dating pure carbonates, such as speleothems and corals [Edwards et al., 2003, and references therein]. When high precision is not an issue, U–Th dating through laser-ablation MC-ICP-MS (LA-MC-ICP-MS) is an interesting alternative to time-consuming conventional methods, allowing a high throughput and high spatial resolution analyses, which may help selecting the most pristine parts of the carbonate sample. This method can also serve as a screening method before high-precision analyses through MC-ICP-MS method on dissolved samples. Until now, comparatively few studies have used this approach [e.g. Eggins et al., 2005, Potter et al., 2005, Hoffmann et al., 2009, Spooner et al., 2016, Lin et al., 2017, Sharp et al., 2019]. Recently, Martin et al. [2022] developed a new method using a single collector plasma source sector field mass spectrometer and a femtosecond laser (fsLA-ICP-SFMS) to perform U–Th analyses on carbonate samples. This method allows mapping of U and Th isotopes used for dating and correction of potential detrital contamination.

We report here the results obtained by LA-MC-ICP-MS on coral samples found in a sedimentary core from the Tunis lagoon (Tunisia). While all analyses of the pristine aragonite coral branches give coherent ages conform to the stratigraphy, we show that a thin overgrowth of Mg-calcite, corresponding to a bio-carbonate secreted by a coralline alga, is characterized by an exceptional enrichment in $^{234}$U and $^{230}$Th, well beyond the closed-system domain in the U–Th evolution diagram. Bulk analysis by dissolution of the coral sample might thus have given an older age than the actual one. In this study, we discuss open-system models able to explain these results.

## 2. Geological setting

The region along the Gulf of Tunis, on the NE coast of Tunisia, is characterized by the presence of several sebkhas and one lagoon (Figure 1), which were isolated from the open Mediterranean Sea through the formation of a sandy lido. The main sediment contributor is Oued Medjerda to the North, and, to a lesser extent, Oued Meliane to the South [Zaara Ben Mosbah et al., 2010, 2017]. While the present mouth of Oued Medjerda in the Gulf of Tunis is located around 36 km north of Tunis, ancient courses flowed further South, just north of the present day Ariana sebkha. The Tunis area is characterised by Oligo-Miocene NW-SE normal faults, which were sometimes reactivated during the Early Quaternary as strike slip faults [Ben Ayed et al., 1985]. In a sustained effort to document the sedimentation and faunal evolution during the late Quaternary, several cores were drilled around the Ariana sebkha [Zaara Ben Mosbah et al., 2010], and the Tunis lagoon [Zaara Ben Mosbah et al., 2017]. Their locations are indicated on the map of Figure 1. The present work was undertaken to define the chronology of the LS1 sedimentary core drilled on the southern border of the Tunis lagoon. A full description of the sedimentology, macro- and micro-fauna of this core can be found in the paper by Hajji et al. [2023].

## 3. Samples and method

Loose coral branches of the species *Balanophyllia Regia* were recovered at several levels from the 40 m long LS1 sedimentary core [Zaara Ben Mosbah et al., 2017, Hajji et al., 2023] (Figure 2). They were extracted from the silty-clayed and sometimes sandy sediment, and carefully cleaned with distilled water. The coral fragments were sawed into cm-long sections, ultrasonically cleaned in ultra-pure water and dried at 60 °C. They were then included in an araldite-type resin, using plastic moulds of 25 mm internal diameter manufactured by Struers™. After consolidation, the surface was polished, and a final ultrasonic cleaning was applied before analysis.

Laser ablation isotopic analyses were done using a Neptune$^+$ MC-ICP-MS manufactured by ThermoFisher Scientific, interfaced with a Teledyne G2 excimer laser delivering a short pulse, 193 nm laser beam (AETE-ISO analytical platform of the OSU OREME, University of Montpellier). Analyses were carried out using a laser spot size of 150 µm in diameter. The power of the laser was adjusted to 7 J/cm$^2$, with a frequency of 10 Hz. Ablation experiments were conducted in a two-volume Helex cell. Samples
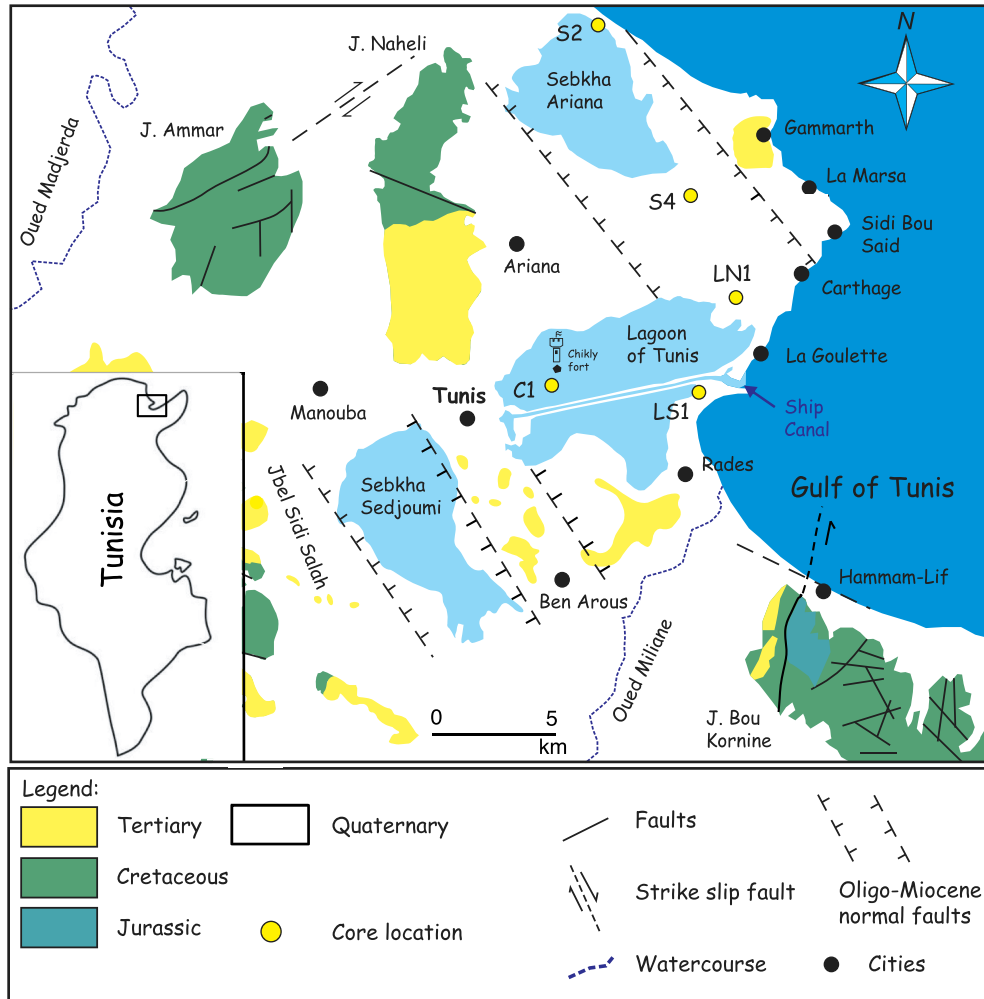
**Figure 1.** Geological map of the coastal area along the Gulf of Tunis [NE Tunisia; after Ben Ayed et al., 1985 and Hajji et al., 2023]. The analysed samples come from the LS1 core, on the SE border of the Tunis lagoon.

and reference materials were ablated under pure Helium (c. 1 L/mn), which was mixed with $N_2$ gas flow (c. 10 ml/mn) after the ablation cell, and later with Ar just before entering the plasma source.

The main analytical parameters are summarized in Table 1, together with the cup configuration used for U–Th analyses. $^{238}U$ signals of around 30 mV (with a $10^{11}$ $\Omega$ resistor) were obtained for coral samples. Due to the low-intensity of $^{234}U$ and $^{230}Th$ signals, both isotopes require the use of SEM, and the analysis cannot be done in a single static mode. We used essentially the same method described by Eggins et al. [2005]. The analyses were made in

a raster mode (2 mm-long track with a speed of 10 µm/s, and a ~1 s integration time). In a first step, $^{230}Th$ is measured on the SEM, $^{235}U$ on the H3 cup, and $^{238}U$ on the H4 cup. With the above parameters, 200 $^{230}Th/^{238}U$ ratios are measured. Then, in a second step, using the same track as previously, $^{234}U$ is measured on the SEM, $^{232}Th$ on the L1 cup (with a $10^{12}$ $\Omega$ resistor), $^{235}U$ on the H1 cup and $^{238}U$ on the H2 cup. During this step, 200 $^{234}U/^{238}U$ ratios are measured. In order to correct for instrumental mass bias, elemental fractionation between U and Th isotopes, and SEM-Faraday cup gain, the bracketing standard method was used. The standard used is

**Figure 2.** Coral branches of Balanophyllia Regia embedded in the sediment of core LS1 from the Tunis lagoon [Hajji et al., 2023]. The pen is 14 cm long.

a calcite sample from a speleothem collected in the Wilder Mann cave in Austria [WM1 sample, Meyer et al., 2009]. This speleothem has been dated by the U–Pb method at 2 Ma [Meyer et al., 2009], and secular radioactive equilibrium was verified by Hoffmann et al. [2007] and Cheng et al. [2013]. Analyses of the WM1 standard were intercalated between 2 to 4 coral sample analyses. Before laser ablation, background counts of the SEM were measured at masses 230 and 234. The backgrounds at masses 230 and 234 are usually around 1 count/s and <0.2 count/s respectively. Background at mass 234 is negligible compared to the $^{234}$U signals, generally ≥100 cps, and within measurement uncertainties, but background at mass 230 is not, since $^{230}$Th signals as low as 20 cps are measured and a background correction has to be applied.

Tailing effects of $^{232}$Th mass on $^{230}$Th, and $^{238}$U mass on $^{234}$U should also be considered. However as $^{232}$Th contents in aragonite are very low (a few ppb), the tailing of the $^{232}$Th peak under mass 230 is negligible, even without the retarding potential quadrupole (RPQ) filter. Without the RPQ, the contribution of the $^{238}$U tail to mass 234 ($^{238}$U$_{tail}$/$^{234}$U) is $2.3 \times 10^{-7}$. With $^{234}$U/$^{238}$U atomic ratios between 5 and $6 \times 10^{-5}$, the correction on the measured $^{234}$U/$^{238}$U ratio is less than 0.5%. Moreover, as $^{234}$U/$^{238}$U ratios of aragonite samples and of the WM1 standard are all very similar, the cor-

rection on the ($^{234}$U/$^{238}$U) activity ratio is less than 1‰, largely within measurement uncertainties. Tailing corrections were slightly larger for the C28–O sample because of its higher Th content and high ($^{234}$U/$^{238}$U) ratio, compared to WM1: 2‰ and 3.4‰ for ($^{234}$U/$^{238}$U) and ($^{230}$Th/$^{238}$U) ratios respectively.

($^{234}$U/$^{238}$U) and ($^{230}$Th/$^{238}$U) activity ratios are simply calculated by dividing the respective interpolated $^{238}$U/$^{230}$Th and $^{238}$U/$^{234}$U atomic ratios of the WM1 standard by those measured on samples, since WM1 is in secular radioactive equilibrium (e.g. ($^{230}$Th/$^{238}$U)$_{sample}$ = $^{238}$U/$^{230}$Th$_{WM1}$/$^{238}$U/$^{230}$Th$_{sample}$ × 1).

In addition, trace element contents of one of the C28 coral branch and its overgrowth (C28–O) were performed *in-situ* by laser ablation ICP-MS using a single collector, sector field, Element XR ICP-MS (ThermoFisher Scientific) and the same laser as described above (Teledyne G2). Analyses were performed using a 85 μm spot size, a 5 Hz frequency and a 5.5 J/cm$^2$ energy density. Total analysis time was 80 s with the first 40 s used for background measurement before sample ablation. Synthetic glass NIST 612 was used for external calibration [values after Pearce et al., 1997]. Internal standard was CaO (56% stoichiometric value) and accuracy of the analyses was monitored using the fused glass standard BIR-1G (values taken from GEOREM preferred values) and the WM1 matrix matching reference material [Meyer et al., 2009]. Data evaluation was done with the software package Glitter [Van Achterberg et al., 2001].

## 4. Results and discussion

Analytical results are reported in Table 2 (U–Th isotopic analyses) and Table 3 (trace element concentrations of coral branch C28 and its border C28–O).

For U–Th isotopic analyses, except for the single C28–O analysis, all other coral data represent weighted averages of several laser-ablation analyses of each coral sample (4 to 6 analyses). It should be noted that the U contents quoted in Table 2 are only indicative. They are calculated by comparing the $^{238}$U signals of the sample and WM1 standard, and taking into account the average U content measured on our piece of WM1 standard (22.7 ± 2.4 ppm, calibrated against the NIST 612 standard). However, the U distribution in the WM1 calcite is not uniform, and we estimate that the precision on the U contents in our coral samples is not better than 10%.

**Table 1.** Laser-ablation parameters and Neptune Plus cup configuration used for the analyses of coral samples

| Laser system | Spot size (μm) | Repetition rate (Hz) | Energy (J/cm$^2$) | Length of line scan (mm) | Line scan speed (μm/s) | Ar sample gas flow (L/min) | He carrier gas flow (L/min) | N$_2$ add gas flow (L/min) |
|---|---|---|---|---|---|---|---|---|
| | 150 | 10 | 7 | 2 | 10 | | 1 | 0.010 |
| Cup configuration | L3 | L2 | L1 ($10^{12}\,\Omega$) | C/SEM | H1 | H2 | H3 | H4 |
| Line 1 | | | | $^{230}$Th | | ($^{234}$U) | $^{235}$U | $^{238}$U |
| Line 2 | | | $^{232}$Th | $^{234}$U | $^{235}$U | $^{238}$U | | |

**Table 2.** U–Th results for 5 aragonitic corals from the Tunis lagoon and the Mg-calcite border of the C28 sample (C28–O)

| Samples | Depth (m) | Number of analyses | U (ppm) | ($^{230}$Th/$^{238}$U) | ($^{234}$U/$^{238}$U) | Age (ka) | OS Age (ka) | ($^{234}$U/$^{238}$U)$_0$ |
|---|---|---|---|---|---|---|---|---|
| C26.8 | 26.8 | 5 | 1.95 | 0.830 ± 0.014 | 1.065 ± 0.006 | 160.3 ± 6.5 | 182 ± 9 | 1.102 ± 0.009 |
| C28 | 28 | 5 | 1.98 | 0.872 ± 0.029 | 1.078 ± 0.013 | 174 ± 15 | 183 ± 21 | 1.127 ± 0.020 |
| C28–O | 28 | 1 | 1.49 | 2.044 ± 0.072 | 1.406 ± 0.020 | | | |
| C32.5 | 32.5 | 5 | 2.14 | 0.889 ± 0.030 | 1.080 ± 0.007 | 181 ± 16 | 187 ± 16 | 1.133 ± 0.012 |
| C36.4 | 36.4 | 4 | 3.02 | 0.891 ± 0.015 | 1.079 ± 0.013 | 183 ± 10 | 189 ± 19 | 1.132 ± 0.020 |
| C38.2 | 38.2 | 4 | 2.62 | 0.906 ± 0.038 | 1.079 ± 0.007 | 191 ± 21 | 196 ± 21 | 1.135 ± 0.013 |

Ages and ($^{234}$U/$^{238}$U)$_0$ initial ratios are calculated using the IsoplotR program [Vermeesch, 2018], with the decay constants given by Cheng et al. [2013]. All reported errors are 2σ. U contents are only indicative (±10%, see text). OS ages are open-system ages calculated with the model proposed by Thompson et al. [2003] assuming that all coral samples initially incorporated U with the seawater ($^{234}$U/$^{238}$U) ratio of 1.145.

The U contents (2 to 3 ppm) of the analysed corals are well within the range found in aragonite corals [1.5 to 4 ppm; Scholz and Hoffmann, 2008]. Th contents are usually in the ppb range in aragonite corals. The calculated ($^{238}$U/$^{232}$Th) and ($^{230}$Th/$^{232}$Th) activity ratios are both higher than 1000 in most analyses of our coral samples (>100 in sample C36.4), and no detrital correction has been applied. The relative internal precisions on ($^{230}$Th/$^{238}$U) and ($^{234}$U/$^{238}$U) ratios (1 standard error on the average of 200 ratios for a single analysis) are 1.5–2% and 0.7% respectively. These values are comparable to those reported in other studies using LA-MC-ICP-MS for U–Th dating of carbonates [e.g. Eggins et al., 2005]. However, the uncertainties reported in Table 2 takes into account the dispersion of the ratios for several analyses of a given coral sample, giving a more realistic estimate of the true uncertainties.

($^{230}$Th/$^{238}$U) and ($^{234}$U/$^{238}$U) activity ratios in the analysed coral samples from various depths range from 0.830 to 0.906 and from 1.065 to 1.080 respectively. A notable exception is the sample C28–O, which represents an overgrowth on a section of coral C28, and has very high ratios of 2.044 and 1.406 respectively. This sample will be discussed later in Section 4.2.

## 4.1. *Ages and ($^{234}$U/$^{238}$U) initial ratios*

The ages and initial ($^{234}$U/$^{238}$U)$_0$ ratios were calculated using the IsoplotR program [Vermeesch, 2018], based on the original Isoplot program developed by Ludwig [1999]. They are reported in Table 2 and in the evolution diagram of Figure 3a. Ages range from 191 ka at 38.2 m depth to 160 ka at 26.8 m depth, decreasing towards the top of the core in agreement with the stratigraphy. ($^{234}$U/$^{238}$U)$_0$ initial ratios are

**Table 3.** Comparison of the minor and trace element contents of coral aragonite and the outer Mg-calcite border produced by a coralline alga (C28–O sample)

| Element | Concentration in Aragonite (ppm) | Concentration in Mg-calcite (ppm) | $C_{Mg\text{-}calcite}/C_{aragonite}$ |
|---|---|---|---|
| B | 27.7 | 18.2 | 0.66 |
| Mg | 0.101% | 4.15% | 41.0 |
| Ca | 39.4% | 34.2% | 0.87 |
| Sr | 7340 | 1460 | 0.20 |
| Ba | 12.7 | 10.0 | 0.79 |
| Al | <DL | 21.3 | |
| Mn | 0.87 | 167 | 188 |
| Fe | 158 | 1280 | 8.15 |
| Co | 0.36 | 0.88 | 2.41 |
| Cu | 0.24 | 1.40 | 5.85 |
| Zn | 2.57 | 9.59 | 3.74 |
| Y | 0.09 | 2.85 | 32.5 |
| La | 0.20 | 0.88 | 4.41 |
| Ce | 0.54 | 2.62 | 4.83 |
| Pr | 0.051 | 0.25 | 4.91 |
| Nd | 0.23 | 1.12 | 4.94 |
| Sm | 0.028 | 0.32 | 11.5 |
| Eu | 0.0047 | 0.091 | 19.2 |
| Gd | 0.019 | 0.40 | 20.9 |
| Tb | 0.0031 | 0.068 | 22.0 |
| Dy | 0.011 | 0.42 | 37.9 |
| Ho | 0.0014 | 0.088 | 62.5 |
| Er | 0.0068 | 0.25 | 36.6 |
| Tm | 0.0007 | 0.037 | 49.8 |
| Yb | 0.0077 | 0.27 | 34.6 |
| Lu | 0.0004 | 0.036 | 83.2 |
| Pb | 0.036 | 1.31 | 36.8 |
| Th | 0.0037 | 0.147 | 39.7 |
| U | 1.84 | 1.48 | 0.80 |

Reported values are averages of 4 analyses for both aragonite and Mg-calcite.

compatible with the seawater ratio of 1.145 [Chen et al., 1986], or 1.1468 [Andersen et al., 2010], within $2\sigma$ uncertainties, except for the youngest C26.8 coral which has a slightly lower ratio (1.102 ± 0.009). The latter could be the result of a change from open-sea to lagoon conditions, with a greater influence of seepage groundwater. But it could also indicate an opening of the U–Th system, as suggested by the rather large age difference between corals sampled at 28 and 26.8 m depth (~14 ka). It might be signifi-cant that all the other samples, although close to the seawater curve, do plot slightly below this curve (Figure 3a), suggesting a possible minor open-system be-haviour. Thompson et al. [2003] proposed an open-system model that explains data below the seawater evolution curve by losses of $^{234}$Th ($^{234}$U) and $^{230}$Th recoil nuclei. Correcting the ages using their model gives ages increasing from 182 ka at 26.8 m to 196 ka at 38.2 m depth. These open-system ages are also reported in Table 2. As expected, only the coral age

at 26.8 m is significantly different from its closed-system age (182 ka instead of 160 ka). All coral samples belong to the end of isotope stage 7 [or sub-stages of isotope stage 6; Railsback et al., 2015], confirming earlier alpha-spectrometry results obtained on samples from the Ariana sebkha and Tunis lagoon [Zaara Ben Mosbah et al., 2010, 2017]. These new ages better constrain the stratigraphic correlations along the coasts of the Gulf of Tunis, and the evolution of the Tunis lagoon from an open-sea to a closed lagoon environment. A thorough discussion is to be found in the paper by Hajji et al. [2023].

## 4.2. *The C28–O sample: Evidence for exceptional open-system behaviour*

The C28–O sample corresponds to a light brown outer layer surrounding the white aragonite skeleton of a few of the C28 coral branches (inset of Figure 3b). This laminated overgrowth is made of successive thin layers (25 to 40 µm thick) of calcite with a palisade texture (Figure 4). Such a laminated structure results from the activity of coralline red algae, belonging to the Lithophyllum pustulatum species [Braga, personal communication; Braga and Aguirre, 1995]. The absence of any apparent discontinuity between the aragonitic coral skeleton and the calcite crust suggests that the coralline algae developed on the living coral, or soon after its death in the marine environment.

Minor and trace element analyses were carried out *in-situ* using LA-ICP-MS on this outer layer (Table 3), and the results compared to those obtained on the inner aragonite coral skeleton. The calcite outer layer is enriched in Mg (17 mol%) and depleted in Sr and, to a lesser extent, Ba compared to the aragonite. Indeed Sr and Ba are easily substituted to Ca in aragonite, but not in calcite, contrary to Mg. Mg-calcite is the primary bio-mineral commonly produced by coralline red algae in Neogene seawater [e.g. Ries, 2010]. The low Al content (21 ppm on average) in the Mg-calcite layers shows the absence of significant contamination by detrital clay minerals [0.02% assuming an Al content of 11% in the clay component as done by Henderson et al., 2001]. Most of the other analysed elements are enriched in the Mg-calcite compared to the aragonite. This is true for REE, particularly for the heavy REE and Y, and also for divalent transition elements, like Mn, Fe, Co, Cu, Zn. The large enrichment
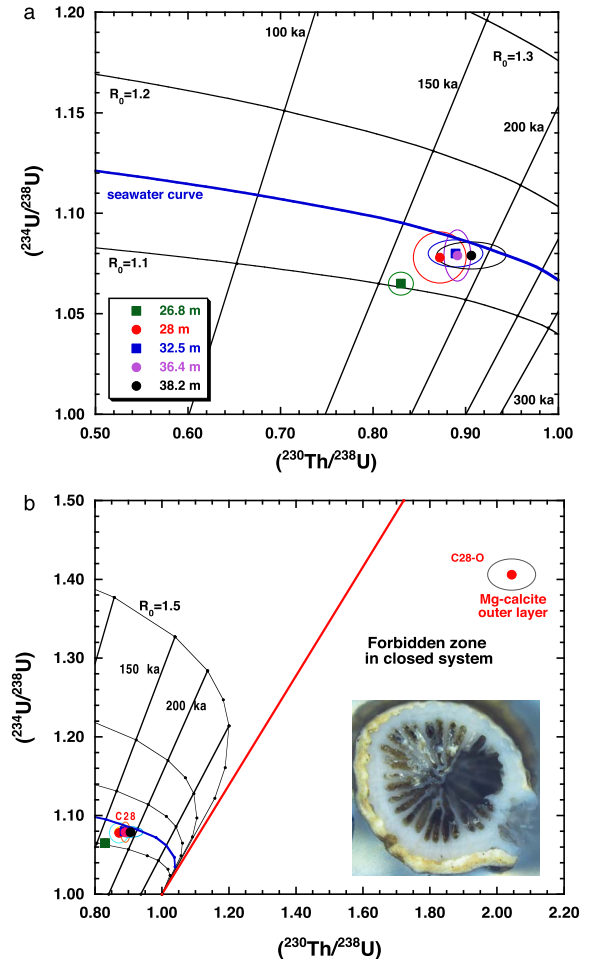


**Figure 3.** (a) Data for the coral samples reported in the $(^{234}U/^{238}U)$–$(^{230}Th/^{238}U)$ evolution diagram. Four of the five samples plot on the seawater evolution curve (in blue) within $2\sigma$ uncertainties (see text for discussion). (b) Enlarged U–Th evolution diagram that shows the data for the Mg-calcite border of the C28 coral sample, well into the "forbidden" zone for a closed-system evolution (limited by the red line). Inset: a polished section of a C28 coral branch, around 6 mm in diameter. The coral skeleton is made of aragonite while the light-brown outer layer is made of Mg-calcite resulting from the activity of an encrusting coralline red alga (see text for discussion).

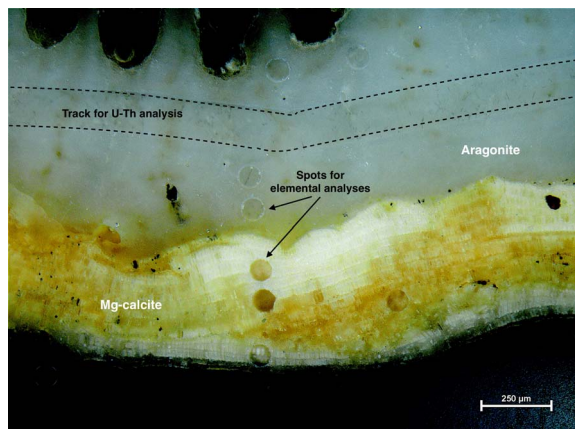in Y and HREE in the Mg-calcite is probably due to the close similarity of their ionic radii with that of

**Figure 4.** Close-up view of the C28 aragonite skeleton and the Mg-calcite outer layer. The dashed lines delineate the laser track used for U–Th analysis by LA-MC-ICP-MS in the aragonite, while the circles indicate spots used for trace element analyses by LA-HR-ICP-MS.

$Ca^{2+}$ (e.g. Lu, Y and Ca have the same ionic radius of 0.93 Å). The charge balance needed to incorporate these trivalent ions can be provided by the substitution of $CO_3^{2-}$ by $BO_3^{3-}$, one of the boron oxyanions found in biogenic calcite [Balan et al., 2016]. Mn and Fe are strongly enriched in the Mg-calcite (Table 3). The presence in and between the Mg-calcite layers of dark inclusions and brown deposits suggests that these elements might be partly included in Fe–Mn hydroxides. Th content is also relatively high (0.15 ppm), with a U/Th ratio of 10, and is unlikely to derive exclusively from a detrital clay component in view of its very small proportion as indicated by the low Al content of the Mg-calcite layer. Conversely, Th might have been scavenged directly from seawater at the time of Mg-calcite production by the coralline algae. In that case, a significant amount of $^{230}$Th could have been initially introduced in the calcite, as the ($^{230}$Th/$^{232}$Th) activity ratio in surface seawater can be much higher than the "crustal" ratio of about 0.8 usually assumed for a detrital component in radioactive equilibrium [e.g. Henderson et al., 2001, Roy-Barman et al., 2002].

The most striking feature is the very high ($^{230}$Th/$^{238}$U) and ($^{234}$U/$^{238}$U) ratios found in this calcite outer layer (2.044 and 1.406 respectively). When plotted on the U–Th evolution diagram (Figure 3b), the representative data point clearly falls in

the "forbidden" zone, and cannot be explained by a closed-system evolution. Open-system behaviour of the U–Th system in carbonates produced by coralline algae has already been reported by Linge et al. [2008]. None of their data, however, falls into the forbidden zone. To our knowledge, there is no mention of other carbonate samples plotting so far away of the closed-system limit in the U–Th evolution diagram.

Numerous open system-models were developed to explain high ($^{234}$U/$^{238}$U) and associated anomalous ($^{230}$Th/$^{238}$U) ratios in marine carbonates such as corals, aragonite-rich sediments or mollusc shells. Most of them are referenced in the Cheng et al.'s paper [1998] that extends the discussion to the $^{235}$U–$^{231}$Pa system. These authors considered several processes of episodic or continuous loss or gain of $^{238}$U, $^{234}$U and/or $^{230}$Th, and showed that the true age of altered corals can sometimes be derived from the intersection of their linear array and the seawater evolution curve in the U–Th diagram, in a similar way as in the U–Pb Concordia diagram. Yehudai et al. [2017] modelled the effect of recrystallization of coral aragonite to calcite to infer U–Th ages of uplifted marine terraces in the Gulf of Aqaba.

Scholz et al. [2004] devised a model to explain ($^{234}$U/$^{238}$U)$_0$ initial ratios higher than the seawater value in altered corals. They assume that corals of the same age undergo various degrees of U gain with a given ($^{234}$U/$^{238}$U) ratio higher than the seawater value of 1.145, followed by U loss in the same proportions. Their model also results in a linear array in the U–Th evolution diagram, with the true age obtained as described above for the Cheng et al.'s [1998] model.

Another category of open-system models only involves enrichments of the samples in $^{234}$U and $^{230}$Th by alpha-recoil processes from an external source, usually the surrounding sediment [Henderson et al., 2001, Villemant and Feuillet, 2003]. The most complete model was proposed by Thompson et al. [2003]. All these models however were designed to explain coral data that do not plot on the seawater evolution curve in the U–Th evolution diagram, but still are, for most of them, in the closed-system field (i.e. an apparent age could be calculated). Whether they can explain the data of our Mg-calcite sample, which plot well outside the closed-system field, is the purpose of the following discussion.

The model proposed by Scholz et al. [2004] involves a post-crystallization addition of U with a high $(^{234}U/^{238}U)$ ratio, necessarily higher in our case than the measured ratio of 1.41. If this U addition occurred shortly after the formation of the coral aragonite skeleton and the sub-contemporaneous coralline alga Mg-calcite, with an age of 174 ka, the initial $(^{234}U/^{238}U)_0$ ratio of the added U should be higher than 2.30. Such values are commonly found in continental groundwater [e.g. Osmond and Cowart, 1992]. Marine pore waters, however, do not show such high ratios [e.g. Maher et al., 2004], and it is difficult to envision how a terrestrial groundwater could have percolated through the deeply buried and relatively impermeable marine sediment. For this reason, we have preferentially tested the model proposed by Thompson et al. [2003], that does not require a fluid with a high $(^{234}U/^{238}U)$ ratio, but a source enriched in U that provides $^{234}Th$ ($^{234}U$) and $^{230}Th$ recoil nuclei to the Mg-calcite.

The results of the model are graphically represented in the U–Th evolution diagram of Figure 5. The source is assumed to have the seawater $(^{234}U/^{238}U)$ ratio of 1.145. The fraction of $^{234}Th$ recoil nuclei remaining in the source ($f_{234}$) is set at 0.95. This implies a $f_{230}$ of 0.9421 [Villemant and Feuillet, 2003]. Evolution curves of $(^{230}Th/^{238}U)$ and $(^{234}U/^{238}U)$ ratios are drawn for different values of R (with R = $f \cdot [U]s/[U]c$, where $f$ is the fraction of recoiling nuclei that is actually added to the Mg-calcite and subscripts $s$ and $c$ apply to the source and the Mg-calcite respectively) according to Equations (20) and (21) in Thompson et al. [2003]. The straight lines are open-system isochrons. The limiting open system straight line for an infinite time is shown on the graph and compared to the closed system limit. Its slope only depends on the $f_{234}$ value [Equation (23) in Thompson et al., 2003]. It is clear that the model can explain data that plot in the forbidden zone of the closed system. However this model of continuous addition of recoil nuclei implies that the data point(s) should plot on an isochron corresponding to the age of the beginning of the process. In our case, the addition of recoil nuclei could not be older than the age of the coral, i.e. 174 ka ($\pm$15 ka). As illustrated in Figure 5, the Mg-calcite data fall to the right-hand side of this isochron (or even to the right of a 204 ka isochron, taking into account the maximum age based on the uncertainty of the

open-system age). The $(^{234}U/^{238}U)$ ratio of 1.406 can be reached after 174 ka with a R ratio of 16.4, but the $(^{230}Th/^{238}U)$ ratio is still lower (1.877) than the measured value of 2.044. There are two possible explanations for this discrepancy. One involves the presence of a significant amount of initial $^{230}Th$ incorporated in the Mg-calcite. In order to obtain the measured ratios in 174 ka, an initial $(^{230}Th/^{238}U)_0$ ratio of 0.82 is required. If $^{230}Th$, together with $^{232}Th$ were directly scavenged from seawater, this would imply an initial $(^{230}Th/^{232}Th)_0$ ratio of about 25, a value much higher than those usually measured in surface seawater [<10; e.g. Roy-Barman et al., 2002, Anderson et al., 2012]. Alternatively, the Mg-calcite might have experienced a recent U loss (8.2%), increasing its $(^{230}Th/^{238}U)$ ratio, without affecting the $(^{234}U/^{238}U)$ ratio.

The most severe constraint of this model is that it requires a high R ratio, i.e. a source highly enriched in U. Assuming that half of the recoil nuclei escaping from the source are introduced in the Mg-calcite, i.e. $f$ = 0.5, the U content of the source should be around 50 ppm. Such high U contents are not unusual in black shales rich in organic material [e.g. Bogdanov et al., 1999]. We suggest that organic tissue of the coralline red algae might have played an essential role in scavenging U from seawater. Algae are indeed well known for their capacity to absorb trace elements like U, and they have been used, for example, to remove U from mining waste waters [Kalin et al., 2005]. On the other hand, Amiel et al. [1973] used the fission track method to analyse U in organic matter extracted from a coral skeleton, and estimated that the U content in organic filaments was between 40 and 70 ppm. A recent paper by De Carvalho et al. [2022] demonstrates that encrusting algae of the genus Lithophyllum produces Mg-calcite inside the cell walls from its earlier development stages.

A thin organic algal tissue enriched in U might offer the ideal conditions to provide recoil nuclei to the growing Mg-calcite layers. After the death of the coralline algae and their burial in the reduced zone of the sediment, U is probably further scavenged and stabilized in its tetravalent oxidation state, becoming a long-lasting source of $^{234}Th$ ($^{234}U$) and $^{230}Th$ recoil nuclei. Ultimately this organic matter will be decomposed and its U lost, leaving only the Mg-calcite enriched in recoil nuclei, while their source has eventually disappeared. If this model is valid,
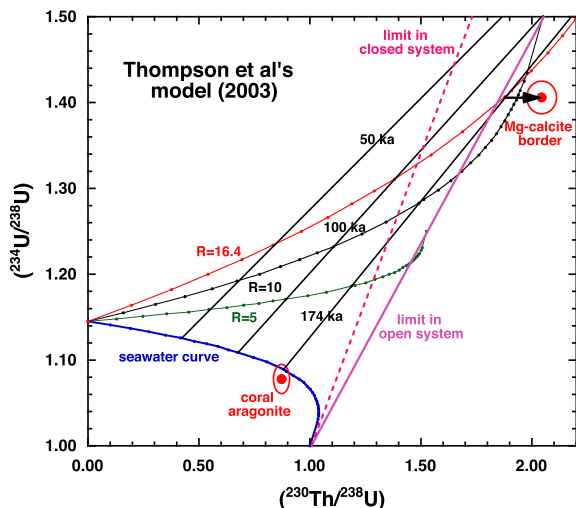
**Figure 5.** The open-system model proposed by Thompson et al. [2003] in the U–Th evolution diagram. Several curves are shown for different values of R, proportional to the ratio of the U contents in the source of recoil nuclei and in the gaining Mg-calcite. Straight lines are open-system isochrons. A 174 ka evolution with an R = 16.4 can explain the $(^{234}U/^{238}U)$ ratio of the Mg-calcite but not exactly its $(^{230}Th/^{238}U)$ ratio. This could result from a recent U loss (black horizontal arrow on the graph). The limits (when *t* tends towards infinity) for open and closed systems are also indicated (full and dashed lines respectively). See text for a detailed discussion.

then the source of recoil nuclei is not to be looked for outside the biologically produced carbonate, but inside it. The main difference between coral aragonite, that often evolves as a closed system and Mg-calcite produced by encrusting coralline algae would reside in the different spatial connections between organic matter and carbonate in those two bio-minerals, and their respective ability to allow U-loss during decay of organic matter.

This model remains speculative, however, and further studies are needed to decipher the behaviour of the U–Th system between organic tissue and carbonates produced by bio-mineralisation. In view of its strong potential to concentrate U, organic matter is likely to be implied in the disturbances that can affect the U–Th system.

## 5. Conclusions

This study confirms that LA-MC-ICP-MS can be successfully applied to date marine carbonates such as corals. Although much less precise than U–Th analyses by TIMS or MC-ICP-MS on dissolved samples, LA-MC-ICP-MS provide stratigraphically coherent results, as demonstrated by our data on coral fragments from a core of the Tunis lagoon. Their ages (from ca 200 to 180 ka) show that this sedimentary sequence was deposited during the end of isotope stage 7 (penultimate Interglacial).

LA-MC-ICP-MS analyses are especially useful when small parts of the samples require particular attention. This is illustrated in our study by the presence around a coral branch of a Mg-calcite border, that was produced by a coralline red alga. Contrary to the aragonitic coral skeleton, that remained a closed-system, the Mg-calcite border is strongly enriched in $^{234}U$ and $^{230}Th$, requiring open-system processes.

The Mg-calcite data are tentatively explained using the Thompson et al.'s [2003] model based on continuous addition of recoil nuclei from an U-enriched source. This model can roughly explain the present data although some additional process like a recent U-loss is probably involved.

The U-rich source required by the model might be provided by thin films of algal organic matter, able to scavenge U from seawater. This organic component could survive in the reduced zone of the sedimentary pile, before being ultimately decomposed, leaving only the Mg-calcite crystals enriched in recoil nuclei.

## Conflicts of interest

Authors have no conflict of interest to declare.

## Acknowledgements

# References

Amiel, A. J., Mille, D. S., and Friedman, G. M. (1973). Incorporation of uranium in modern corals. *Sedimentology*, 20, 523–528.

Andersen, M. B., Stirling, C. H., Zimmermann, B., and Halliday, A. N. (2010). Precise determination of the open-ocean $^{234}$U/$^{238}$U composition. *Geochem. Geophys. Geosyst.*, 11(12), article no. Q12003.

Anderson, R. F., Fleisher, M. Q., Robinson, L. F., Edwards, R. L., Hoff, J. A., Bradley Moran, S., Rutgers van der Loeff, M., Thomas, A. L., Roy-Barman, M., and Francois, R. (2012). GEOTRACES intercalibration of $^{230}$Th, $^{232}$Th, $^{231}$Pa, and prospects for $^{10}$Be. *Limnol. Oceanogr.: Methods*, 10, 179–213.

Balan, E., Pietrucci, F., Gervais, C., Blanchard, M., Schott, J., and Gaillardet, J. (2016). First-principles study of boron speciation in calcite and aragonite. *Geochim. Cosmochim. Acta*, 193, 119–131.

Ben Ayed, N., Viguier, C., and Bobier, C. (1985). Les éléments structuraux récents essentiels de la Tunisie Nord-Orientale. Notes du Service Géologique de Tunisie, n° 47, pages 5–19. Editions du Service Géologique de Tunisie, Tunis.

Bogdanov, R. V., Gerasimov, S. A., Ozernaya, S. A., and Sergeev, A. S. (1999). Organic substance as a collector of recoil atoms $^{234}$Th ($^{234}$U) in black shales. *Czechoslov. J. Phys.*, 49(S1), 65–70.

Braga, J. C. and Aguirre, J. (1995). Taxonomy of fossil coralline algal species: Neogene Lithophylloideae (Rhodophyta, Corallinaceae) from southern Spain. *Rev. Palaeobot. Palynol.*, 86, 265–285.

Chen, J. H., Edwards, R. L., and Wasserburg, G. J. (1986). $^{238}$U, $^{234}$U and $^{232}$Th in seawater. *Earth Planet. Sci. Lett.*, 80, 241–251.

Cheng, H., Edwards, R. L., Murrell, M. T., and Benjamin, T. M. (1998). Uranium-thorium-protactinium dating systematics. *Geochim. Cosmochim. Acta*, 62(21/22), 3437–3452.

Cheng, H., Edwards, R. L., Shen, C.-C., Polyak, V., Asmerom, Y., Woodhead, J., Hellstrom, J., Wang, Y., Kong, X., Spötl, C., Wang, W., and Alexander Jr., E. C. (2013). Improvements in $^{230}$Th dating, $^{230}$Th and $^{234}$U half-life values, and U–Th isotopic measurements by multi-collector inductively coupled plasma mass spectrometry. *Earth Planet. Sci. Lett.*, 371–372, 82–91.

De Carvalho, R. T., Wendt, C. M. C., Willemes, M. J., Da Gama Bahia, R., Farina, M., and Salgado, L. T. (2022). Ontogeny and early steps of the calcification process in coralline algae *Lithophyllum corallinae* (Florideophyceae, Rodophyta). *Front. Mar. Sci.*, 9, article no. 900607.

Edwards, R. L., Gallup, C. D., and Cheng, H. (2003). Uranium-series dating of marine and lacustrine carbonates. In Bourdon, B., Henderson, G. M., Lundstrom, C. C., and Turner, S. P, editors, *Uranium-Series Geochemistry*, volume 52 of *Reviews in Mineralogy and Geochemistry*, pages 363–405. De Gruyter, Berlin, Boston.

Eggins, S. M., Grün, R., McCulloch, M. T., Pike, A. W. G., Chappell, J., Kinsley, L., Mortimer, G., Shelley, M., Murray-Wallace, C. V., Spötl, C., and Taylor, L. (2005). *In-situ* U-series dating by laser-ablation multi-collector ICPMS: new prospects for Quaternary geochronology. *Quat. Sci. Rev.*, 24, 2523–2538.

Hajji, I., Zaara Ben Mosbah, C., Karoui-Yaakoub, N., Condomines, M., Bruguier, O., Temani, R., and Chaabani, F. (2023). Evolution des écosystèmes de la lagune de Tunis du Pléistocène moyen à l'actuel. *Ann. de Paléontol.* (submitted).

Henderson, G. M., Slowey, N. C., and Fleisher, M. Q. (2001). U–Th dating of carbonate platform and slope sediments. *Geochim. Cosmochim. Acta*, 65(16), 2757–2770.

Hoffmann, D. L., Prytulak, J., Richards, D. A., Elliott, T., Coath, C. D., Smart, P. L., and Scholz, D. (2007). Procedures for accurate U and Th isotope measurements by high precision MC-ICPMS. *Int. J. Mass Spectrom.*, 264, 97–109.

Hoffmann, D. L., Spötl, C., and Mangini, A. (2009). Micromill and *in situ* laser ablation sampling techniques for high spatial resolution MC-ICPMS U–Th dating of carbonates. *Chem. Geol.*, 259, 253–261.

Kalin, M., Wheeler, W. N., and Meinrath, G. (2005). The removal of uranium from mining wastewater using algal/microbial biomass. *J. Environ. Radioact.*, 78, 151–177.

Lin, Y., Jochum, K. P., Scholz, D., Hoffmann, D. L., Stoll, B., Weis, U., and Andreae, M. O. (2017). *In-situ* high spatial resolution LA-MC-ICPMS $^{230}$Th/U dating enables detection of small-scale age inversions in speleothems. *Solid Earth Sci.*, 2, 1–9.

Linge, H., Lauritzen, S. E., Mangerud, J., Kamenos, N. A., and Gherardi, J. M. (2008). Assessing the use of U–Th methods to determine the age of cold-water calcareous algae. *Quat. Geochronol.*, 3, 76–88.

Ludwig, K. R. (1999). Using Isoplot/Ex, version 2.01. In *A Geochronological Toolkit for Microsoft Excel*, Berkeley Geochronology Center Special Publication, Berkeley, 1a.

Maher, K., Depaolo, D. J., and Chiu-Fang Lin, J. (2004). Rates of silicate dissolution in deep-sea sediment: *In situ* measurement using $^{234}U/^{238}U$ of pore fluids. *Geochim. Cosmochim. Acta*, 68(22), 4629–4648.

Martin, L., Galy, A., Barbotin, G., Claverie, F., Pons-Branchu, E., Tribolo, C., Mercier, N., and Pécheyran, C. (2022). Isotopic imaging using fsla single-collector ICP-SFMS for direct U/Th dating of small archaeological carbonates. *Anal. Chem.*, 94, 3046–3055.

Meyer, M. C., Cliff, R. A., Spötl, C., Knipping, M., and Mangini, A. (2009). Speleothems from the earliest Quaternary: Snapshots of paleoclimate and landscape evolution at the northern rim of the Alps. *Quat. Sci. Rev.*, 28, 1374–1391.

Osmond, J. K. and Cowart, J. B. (1992). Ground water. In Ivanovich, M. and Harmon, R. S., editors, *Uranium-series Disequilibrium*, pages 290–334. Clarendon Press, Oxford.

Pearce, N. J. G., Perkins, W. T., Westgate, J. A., Gorton, M. P., Jackson, S. E., Neal, C. R., and Chenery, S. P. (1997). A compilation of new and published major and trace element data for NIST SRM 610 and NIST SRM 612 glass reference materials. *Geostand. Newsl.*, 21(1), 115–144.

Potter, E. K., Stirling, C. H., Wiechert, U. H., Halliday, A. N., and Spötl, C. (2005). Uranium-series dating of corals *in situ* using laser-ablation MC-ICPMS. *Int. J. Mass Spectrom.*, 240, 27–35.

Railsback, L. B., Gibbard, P. L., Head, M. J., Voarintsoa, N. R. G., and Toucanne, S. (2015). An optimized scheme of lettered marine isotope substages for the last 1.0 million years, and the climatostratigraphic nature of isotope stages and substages. *Quat. Sci. Rev.*, 111, 94–106.

Ries, J. B. (2010). Review: geological and experimental evidence for secular variation in seawater Mg/Ca (calcite-aragonite seas) and its effects on marine biological calcification. *Biogeosciences*, 7, 2795–2849.

Roy-Barman, M., Coppola, L., and Souhaut, M. (2002). Thorium isotopes in the western Mediter-ranean Sea: an insight into the marine particle dynamics. *Earth Planet. Sci. Lett.*, 196, 161–174.

Scholz, D. and Hoffmann, D. (2008). $^{230}$Th/U dating of fossil corals and speleothems. *Quat. Sci. J.*, 57(1–2), 52–76.

Scholz, D., Mangini, A., and Felis, T. (2004). U-series dating of diagenetically altered fossil reef corals. *Earth Planet. Sci. Lett.*, 218, 163–178.

Sharp, W. D., Tryon, C. A., Niespolo, E. M., Fylstra, N. D., Tripathy-Lang, A., and Faith, J. T. (2019). $^{230}$Th/U burial dating of ostrich eggshell. *Quat. Sci. Rev.*, 219, 263–276.

Spooner, P. T., Chen, T., Robinson, L. F., and Coath, C. D. (2016). Rapid uranium-series age screening of carbonates by laser ablation mass spectrometry. *Quat. Geochronol.*, 31, 28–39.

Thompson, W. G., Spiegelman, M. W., Goldstein, S. L., and Speed, R. C. (2003). An open-system model for U-series age determinations of fossil corals. *Earth Planet. Sci. Lett.*, 210, 365–381.

Van Achterberg, E., Ryan, C. G., Jackson, S. E., and Griffin, W. L. (2001). Data reduction software for LA-ICP-MS: appendix. In Sylvester, P. J., editor, *Laser Ablation-ICP-Mass Spectrometry in the Earth Sciences: Principles and Applications*, volume 29, pages 239–243. Mineralog. Assoc. Canada (MAC) Short Course Series, Ottawa, Ontario, Canada.

Vermeesch, P. (2018). IsoplotR: a free and open toolbox for geochronology. *Geosci. Front.*, 9, 1479–1493.

Villemant, B. and Feuillet, N. (2003). Dating open systems by the $^{238}U–^{234}U–^{230}$Th method: application to Quaternary reef terraces. *Earth Planet. Sci. Lett.*, 210, 105–118.

Yehudai, M., Lazar, B., Bar, N., Kiro, Y., Agnon, A., Shaked, Y., and Stein, M. (2017). U–Th dating of calcite corals from the Gulf of Aqaba. *Geochim. Cosmochim. Acta*, 198, 285–298.

Zaara Ben Mosbah, C., Ben Ismaïl-Lattrache, K., Gueddari, M., and Reyss, J. L. (2010). Évolution biosédimentaire du dépôt quaternaire de la lagune de l'Ariana, Tunisie (une zone humide du Maghreb Nord). *Quaternaire*, 21(2), 181–194.

Zaara Ben Mosbah, C., Hajji, I., Ben Hmida, S., Chaabani, F., Temani, R., Condomines, M., and Martin, C. (2017). Évolution paléo-environnementale et quaternaire de la lagune de Tunis (golfe de Tunis, Tunisie). *Quaternaire*, 28(4), 491–503.